

Nitrate debuts as a dominant contributor to particulate pollution in Beijing: Roles of enhanced atmospheric oxidizing capacity and decreased sulfur dioxide emission

Tian Feng ^{a,e}, Naifang Bei ^c, Shuyu Zhao ^b, Jiarui Wu ^b, Suixin Liu ^b, Xia Li ^b, Lang Liu ^b, Ruonan Wang ^b, Xiu Zhang ^a, Xuexi Tie ^b, Guohui Li ^{b,d,*}

^a Department of Geography & Spatial Information Techniques, Ningbo University, Ningbo, Zhejiang, 315211, China

^b Key Lab of Aerosol Chemistry and Physics, SKLLQG, Institute of Earth Environment, Chinese Academy of Sciences, Xi'an, Shaanxi, 710061, China

^c School of Human Settlements and Civil Engineering, Xi'an Jiaotong University, Xi'an, Shaanxi, 710049, China

^d CAS Center for Excellence in Quaternary Science and Global Change, Xi'an, Shaanxi, 710061, China

^e Institute of East China Sea, Ningbo University, Ningbo, Zhejiang, 315211, China

HIGHLIGHTS

- Increasing nitrate concentration largely offsets the sulfate decrease since 2013.
- Increasing nitrate is mainly due to enhanced AOC and weakened sulfate competition.
- Decreasing AOC is beneficial to mitigate nitrate and PM_{2.5} concentrations.

ARTICLE INFO

Keywords:

Nitrate
Ozone
Atmospheric oxidizing capacity
Sulfate
WRF-Chem

ABSTRACT

Implementation of strict emission mitigation measures since 2013 has significantly changed air pollutants in the Beijing-Tianjin-Hebei region (BTH), China. Observations show that ozone (O₃) concentrations have increased by 62.40% (27.84%) and SO₂ concentrations have decreased by 56.42% (35.07%) during particulate pollution episodes in Beijing (BTH) in the autumn from 2013 to 2015. The measured nitrate concentration in Beijing has increased markedly, which to a large degree offsets the sulfate decrease caused by SO₂ emission mitigation. Using the WRF-Chem model, we demonstrate that the enhanced nitrate formation is primarily attributed to increasing atmospheric oxidizing capacity (AOC) and decreasing sulfate competition for base ions. A 9.41–46.24% (7.58–40.97%) decrease in OH radical (O₃) concentrations in October 2015 reduces nitrate and fine particulate matters (PM_{2.5}) concentrations by 2.51–18.18% and 3.15–18.90% in Beijing, respectively. Based on the scenario in October 2015, if the SO₂ emission increases by 20.00–100.00%, the PM_{2.5} concentration increases by 3.02–11.21%, but the nitrate level decreases by 2.48–21.87% simultaneously. Our results suggest that the nitrate aerosol has become a dominant contributor to particulate pollution in Beijing and that decreasing AOC is critical to mitigate nitrate and PM_{2.5} concentrations.

1. Introduction

Severe particulate pollution has frequently occurred in the Beijing-Tianjin-Hebei (BTH) region of China during recent decades (He et al., 2001; Huang et al., 2014; Wang et al., 2016; F. Wei et al., 1999). Large mass loadings of various inorganic salts and organic matters in fine

particulate matters (PM_{2.5}) during haze days have been reported (Feng et al., 2019; Sun et al., 2013; R. Zhang et al., 2013; G. J. Zheng et al., 2015). High levels of PM_{2.5} rapidly deteriorate air quality and visibility (J. Cao et al., 2012a; Feng et al., 2016; Seinfeld and Pandis, 2006) and exert adverse effects on human health and ecosystem (J. Cao et al., 2012b; Tie et al., 2016). Dense particles in the atmosphere also directly

* Corresponding author. Key Lab of Aerosol Chemistry and Physics, SKLLQG, Institute of Earth Environment, Chinese Academy of Sciences, Xi'an, Shaanxi, 710061, China.

E-mail address: ligh@ieecas.cn (G. Li).

and indirectly impact regional and global climate via their roles in changing incident light and clouds (G. Li et al., 2009; Wu et al., 2019; R. Zhang et al., 2007; Zhao et al., 2017; Zhou et al., 2017).

Since implementation of the “Air Pollution Prevention and Control Action Plan” (APPCAP) in 2013, anthropogenic emissions in BTH have been remarkably mitigated (He et al., 2017; B. Zheng et al., 2018). Observed sulfate aerosols decreased by 33.3%, 29.5%, and 23.1% from 2013 to 2017 in Beijing, Tianjin, and Hebei, respectively (He et al., 2017). However, severe haze events with high levels of PM_{2.5} still frequently occur in BTH (Wang et al., 2016; Q. Zhang et al., 2015; Zhang and Cao, 2015). Wen et al. (2018) have reported increasing trends of the nitrate fraction in PM_{2.5} mass and nitrate/sulfate ratio during the recent decade at 2 sites in adjacent areas of BTH. H. Li et al. (2018) have also observed nitrate-driven particulate pollution in BTH and surrounding areas during summer 2015 and 2017. These studies indicate that nitrate aerosols play an increasingly important role in the particulate pollution over BTH, but the reason for the nitrate increasing trend remains elusive.

The nitrate formation is closely associated with the atmospheric oxidizing capacity (AOC) (Lei and Wuebbles, 2013; Morgan et al., 2010; Poulain et al., 2011; Seinfeld and Pandis, 2006; Stein and Saylor, 2012). Oxidation of nitrogen oxide (NO_x = NO + NO₂) by oxidants such as hydroxyl radical (OH) and ozone (O₃) constitutes the main nitrate formation pathway in ambient air. Enhancement of the AOC or abundance of atmospheric oxidants facilitates the NO_x conversion to form nitrate aerosols. In addition, the competition between sulfate and nitrate for alkali ions, such as ammonium in the atmosphere, also influence nitrate formation (Lei and Wuebbles, 2013; Seinfeld and Pandis, 2006), which depends on total sulfate, total alkali ions, total nitrate, relative humidity and air temperature (Feng et al., 2018).

Recent studies have reported remarkable changes in O₃ and SO₂ concentrations in BTH over the last decade (Cheng et al., 2016; Ma et al., 2016; H. Zhang et al., 2016), especially since implementation of the APPCAP (Cai et al., 2017; G. Li et al., 2017a; Wu et al., 2017). From 2003 to 2015, surface maximum daily average 8 h O₃ concentrations at a rural station in the north of eastern China have increased with a mean rate of 1.13 ± 0.01 ppb y⁻¹ (Ma et al., 2016). Li et al. (2017a) have reported that the O₃ concentration during April–September has increased by 10% from 2013 to 2015 in eastern China. In Beijing, the summertime O₃ concentration has increased by 23% from 2013 to 2015 (Wu et al., 2017). Such an increasing trend of O₃ concentrations reflects enhancement of the AOC. Furthermore, SO₂ emissions in industrial combustion and steel sector have been reduced by 29% and 27% from 2012 to 2017, respectively (Cai et al., 2017), which lowers the sulfate competition for alkali ions and favors the nitrate formation. Additionally, recent studies have shown that the ammonia emissions remained stable from 2013 to 2017 (B. Zheng et al., 2018). Therefore, in this study, we explore the roles of increasing AOC and decreasing sulfate competition in the nitrate formation, while acknowledging the contribution of other factors including variations in relative humidity during haze episodes.

2. Model and methods

2.1. WRF-Chem model and configurations

In this study, we employ a specific version of the WRF-Chem model (Grell et al., 2005) developed by G. Li et al. (2011a; 2012; 2010; 2011b), which includes a flexible gas phase chemical module and the CMAQ aerosol module (Binkowski and Roselle, 2003). The FTUV module (G. Li et al., 2011a; Tie et al., 2003) is incorporated in the model to calculate photolysis rates, with consideration of effects of clouds and aerosols on photolysis. Inorganic aerosols are simulated using the ISORROPIA version 1.7 (Nenes et al., 1998) which calculates the composition and phase state of an ammonium-sulfate-nitrate-chloride-water inorganic aerosol in thermodynamic equilibrium with gas-phase precursors. Besides gas-phase oxidations of SO₂ by OH radicals and stabilized criegee intermediates (sCI), a SO₂ heterogeneous reaction parameterization

proposed by Li et al. (2017b) is also included in the model. Organic aerosols are predicted using the non-traditional secondary organic aerosol module which incorporates the volatility basis-set (VBS) approach (Donahue et al., 2006; Robinson et al., 2007). The dry deposition of chemical species is parameterized using the method in Wesely (1989). The surface and upper air observational wind fields during the study period from China Meteorological Administration (CMA) are assimilated using the four-dimensional data assimilation (FDDA) to give a better model performance in simulating meteorological fields.

We simulate the air pollution over BTH during October 2015 when two severe pollution events occurred in the simulation domain (Fig. 1). The model employs the anthropogenic emission inventory and the diurnal cycles of emission intensity from Zhang et al. (2009) and Li et al. (2017a), which includes emissions from industry, power generation, residential, transportation, and agricultural sources. Fig. 2 shows the spatial distributions of NO_x and SO₂ emissions in the study domain in October 2015. The biogenic emissions are calculated online by the Model of Emissions of Gases and Aerosol from Nature (MEGAN) model (Guenther et al., 2006). A more detailed description of the model configuration is given in Table 1.

2.2. Observations

The observed wind fields for FDDA in the model include wind speed and direction in surface and upper air during the study period, which is retrieved from the available meteorological data in CMA. The pollutant measurements used in this study include hourly observations of O₃, NO_x, SO₂, CO, and PM_{2.5} mass concentrations from ambient monitoring stations of China's Ministry of Environment and Ecology (China MEE). A total of 80 monitoring stations are distributed over the BTH region. The main chemical constituents in PM_{2.5} are measured at the Chinese Research Academy of Environmental Sciences (CRAES) station. Hourly sulfate, nitrate, and ammonium concentrations in PM_{2.5} are measured using the URG 9000 S Ambient Ion Monitor (URG Corporation, Chapel Hill, NC, USA) (Beccaceci et al., 2015; Twigg et al., 2015). Hourly organic carbon (OC) and elemental carbon (EC) concentrations in PM_{2.5}

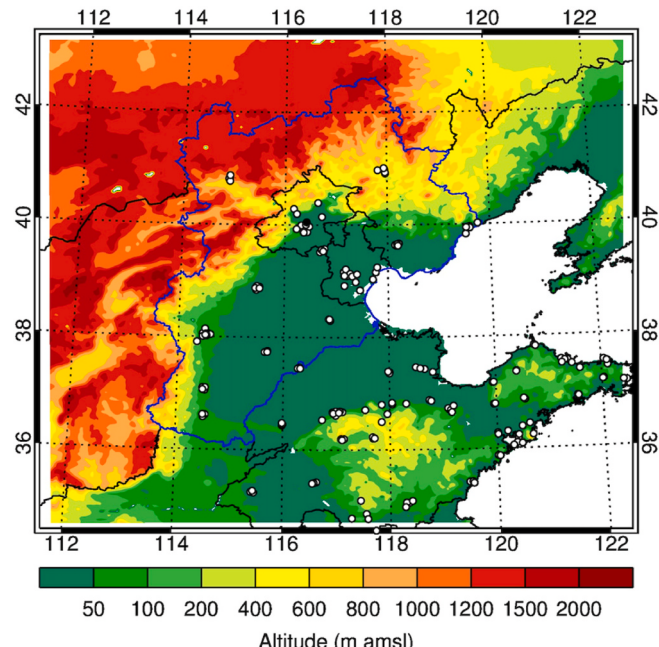


Fig. 1. Map showing the topography of the study area. The white and black dots show the locations of the ambient air quality monitoring sites and the location of the CRAES station. The blue boundary curve presents the BTH area. (For interpretation of the references to this figure legend, the reader is referred to the Web version of this article.)

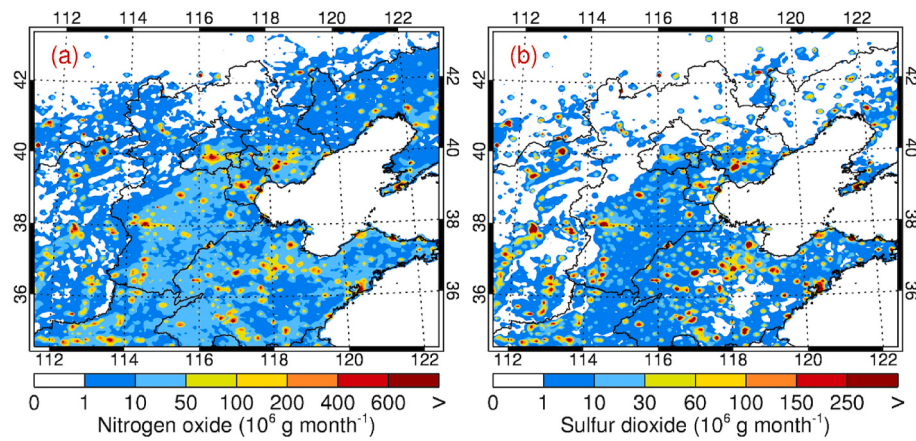


Fig. 2. Geographic distributions of anthropogenic emissions of (A) nitrogen oxide and (B) sulfur dioxide in the simulation domain. The black curves present provincial boundaries in China.

Table 1
Configurations of the WRF-Chem model.

Item	Configuration
Simulation period	October 2015
Domain	The Beijing-Tianjin-Hebei region, China
Domain center	116°E, 38°N
Domain size	1200 km × 1200 km
Horizontal resolution	6 km × 6 km
Vertical resolution	35 vertical levels with a stretched vertical grid with spacing ranging from 50 m near surface, to 500 m at 2.5 km and 1 km above 14 km
Microphysics scheme	WRF Single-Moment 6-class scheme (Hong and Lim, 2006)
Boundary layer scheme	MYJ TKE scheme (Janjić, 2002)
Surface layer scheme	MYJ surface scheme (Janjić, 2002)
Land-surface scheme	Noah land surface model (Chen and Dudhia, 2001)
Longwave radiation scheme	New Goddard scheme (Chou et al., 2001)
Shortwave radiation scheme	New Goddard scheme (Chou and Suarez, 1999)
Meteorological boundary and initial condition	NCEP 1 ° × 1 ° reanalysis data
Chemical boundary and initial condition	MOZART 6-h output (Horowitz et al., 2003)
Anthropogenic emission inventory	SAPRC-99 chemical mechanism emissions (M. Li et al., 2017b; Q. Zhang et al., 2009), base year: 2013 (Fig. 2)
Biogenic emission inventory	MEGAN model developed by Guenther et al. (2006)
Model spin-up time	2 days

are measured simultaneously using a Sunset OC-EC Analyzer (RT-4, Sunset Laboratory, USA) (W. Liu et al., 2018; S. Wei et al., 2014), and an organic aerosol (OA) to OC ratio of 1.8 is adopted to obtain the OA concentration (Aiken et al., 2008; Xing et al., 2013).

2.3. Statistics for model-observation comparison

The mean bias (MB) and dimensionless index of agreement (IOA) are used to evaluate the WRF-Chem model simulations of meteorological fields, gas-phase species, and aerosols.

$$MB = \frac{1}{N} \sum_{i=1}^N (P_i - O_i) \quad (1)$$

$$IOA = 1 - \frac{\sum_{i=1}^N (P_i - O_i)^2}{\sum_{i=1}^N \left(|P_i - \bar{O}| + |O_i - \bar{O}| \right)^2} \quad (2)$$

where P_i and O_i are the simulated and observed variables, respectively. N is the total number of predictions and \bar{O} denotes the average of ob-

servations. IOA has a theoretical range from 0 to 1, with higher values suggesting better agreement between simulation and observation (Willmott, 1981).

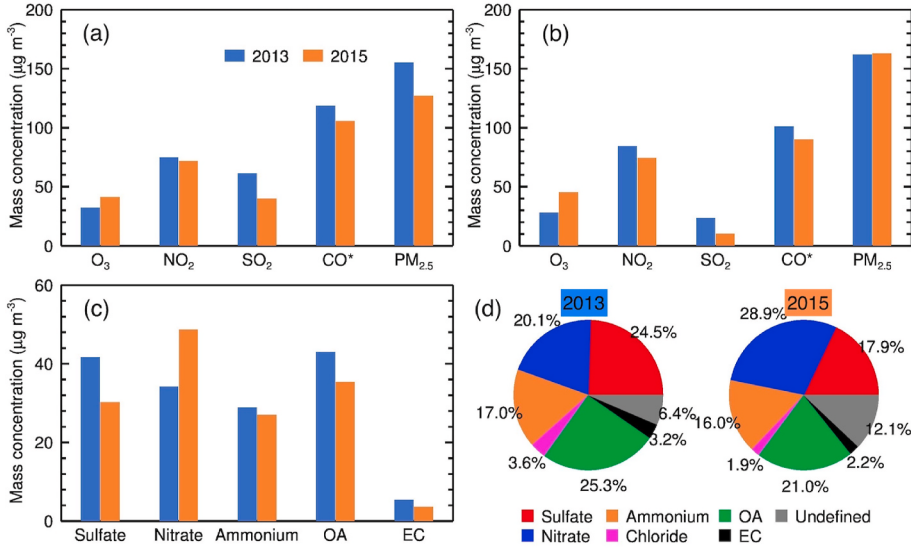
2.4. Model experiments

For discussion convenience, we have defined the REF case without changes of AOC and SO₂ emissions and the results of the REF case have been validated against available observations. Chen et al. (2020) have reported that the measured O₃ (O₃+NO₂) concentration has increased by 49.8% (7.6%) from 2013 to 2019 in Beijing, showing a strong enhancement of the AOC. Meanwhile, the SO₂ emission has decreased by 51.4%, 47.3%, and 28.1% in Beijing, Tianjin, and Hebei, respectively, as a result of the clean air action (He et al., 2017). In consideration of these facts, we design two scenarios of sensitivity simulations to investigate impacts of the variation of AOC and SO₂ emissions on the nitrate formation, while acknowledging the contribution of other factors such as the variations in relative humidity. In the first scenario, five experiments (AOC1-5) are performed to investigate the impact of altering the AOC on atmospheric composition. In these experiments, photolysis frequencies are decreased by 10%–50% with an interval of 10%. In the second scenario, we conduct another five sensitivity experiments (SUL1-5) with SO₂ emissions increased from 20% to 100% with an interval of 20% considering the remarkable decrease in SO₂ levels (Fig. 3a–b).

3. Results and discussion

3.1. Analysis of observed air pollutants

Hourly observations of O₃, NO₂, SO₂, CO, and PM_{2.5} mass concentrations at the national ambient monitoring sites in the autumn of 2013 and 2015 are analyzed. Considering that the heating season generally starts from November 15 in northern China every year, the observations during the particulate pollution episodes with hourly PM_{2.5} concentrations exceeding 75 µg m⁻³ from September 15 to November 14 are selected for analysis in this study. Fig. 3a presents the average concentration of five air pollutants over BTH in the autumn of 2013 and 2015 during pollution episodes. SO₂ concentrations have decreased by 35.1% from 2013 to 2015, showing an effective control of SO₂ emissions since 2013. PM_{2.5} concentrations have decreased by 18.2%, not as significant as that of SO₂. NO₂ concentrations exhibit a slight decreasing trend, with a reduction of about 4.4% from 2013 to 2015. However, the O₃ level has increased by 27.8%, indicating a substantial enhancement of the AOC in BTH during particulate pollution episodes. The reasons for the ozone increase still remain unclear. The decrease in NOx emissions would



weaken NO titration and elevate the O_3 levels. The change in incident solar radiation, partially caused by decreased aerosol concentrations, is probably another candidate. Additionally, the decrease in airborne particulates has been proposed as a potential culprit (K. Li et al., 2018), which leads to a decrease in aerosol surface and hence radical chemistry. Further studies are still in need to uncover the causes.

In general, the air pollutant variations from 2013 to 2015 in Beijing follow those over BTH, except for $PM_{2.5}$ (Fig. 3b). The decrease in SO_2 and NO_2 concentrations is more noticeable in Beijing than that over BTH, attaining 56.4% and 11.9%, respectively. The O_3 concentrations exhibit a significant increasing trend with an enhancement of 62.4%, showing remarkable AOC enhancement in Beijing. The variation of

$PM_{2.5}$ concentrations in Beijing is different from that over BTH, with a slight increase of about 0.5% from 2013 to 2015. We further analyze the variation of main constituents in $PM_{2.5}$ observed at the CRAES site during particulate pollution episodes from 2013 to 2015, to interpret the $PM_{2.5}$ trend in Beijing. Fig. 3c-d shows that sulfate concentrations in Beijing have decreased by 27.3% or $11.4 \mu g m^{-3}$, which corresponds well to the variation of SO_2 , and the sulfate mass fraction in $PM_{2.5}$ has decreased from 24.5% to 17.9%. Concentrations of ammonium aerosols, OA, and EC have also decreased slightly since implementation of the APPCAP. Meanwhile, the nitrate aerosol concentration has increased by 42.5% or $14.5 \mu g m^{-3}$ and its mass fraction in $PM_{2.5}$ has increased from 20.1% to 28.9%. The nitrate aerosol has become a dominant constituent

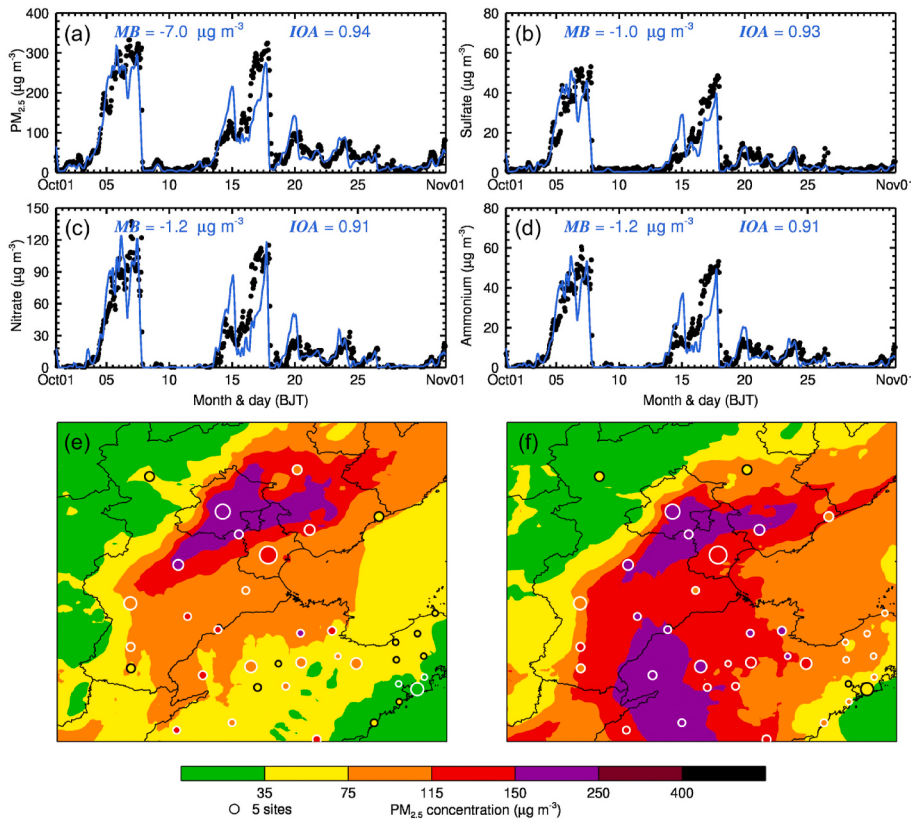


Fig. 4. Modeled (colored shadings) and observed (colored dots) aerosols. (a–d) are diurnal profiles of observed (black dots) and simulated (red curves) $PM_{2.5}$ concentration averaged over the ambient monitoring stations in Beijing, and sulfate, nitrate, and ammonium aerosols in $PM_{2.5}$ at the CRAES site (Fig. 1). (e–f) are the spatial distributions of $PM_{2.5}$ concentrations averaged during two severe particulate pollution episodes in October (5–7 October and 14–17 October). The size of the colored dots presents the number of ambient monitoring stations in each city. (For interpretation of the references to color in this figure legend, the reader is referred to the Web version of this article.)

of PM_{2.5}, and the nitrate increase from 2013 to 2015 offsets the sulfate decrease in Beijing. Therefore, it is imperative to explore the reason for increasing nitrate aerosols to support the design and implementation of emission control strategies in Beijing.

3.2. Validation of model simulation

To probe into the reasons for the increasing nitrate aerosols in Beijing, we need to evaluate the model performance firstly in simulating the atmospheric chemistry. The model simulation is validated using observations of air pollutants over BTH and aerosol constituents in Beijing. Fig. 4a presents the diurnal profiles of the predicted and observed PM_{2.5} concentrations in Beijing during the simulation period. The model successfully captures the two severe particulate pollution episodes in October 2015 with peak PM_{2.5} concentrations exceeding 300 $\mu\text{g m}^{-3}$. The simulated temporal variation of PM_{2.5} concentrations is in good agreement with observations, with an MB of $-7.0 \mu\text{g m}^{-3}$ and an IOA of 0.94. The model also well reproduces the temporal variations of sulfate, nitrate, and ammonium concentrations against measurement at the CRAES site, with IOAs exceeding 0.9 (Fig. 4b-d). It is worth noting that the observed nitrate concentration is extremely high during the severe particulate pollution episodes, reaching around 120 $\mu\text{g m}^{-3}$ and accounting for nearly 40% of the total PM_{2.5} mass (Fig. 4c). Peak sulfate and ammonium concentrations are generally less than 60 $\mu\text{g m}^{-3}$, much lower than nitrate aerosols. Apparently, compared with observations before implementation of the APPCAP (Sun et al., 2012; 2013), the nitrate mass fraction in PM_{2.5} in Beijing has substantially increased in 2015.

The simulated spatial distributions of PM_{2.5} concentrations during the two severe particulate pollution episodes are presented in Fig. 4e-f along with the observations. The model generally performs well in simulating the PM_{2.5} distribution compared to observations in BTH. During the first episode from 5 to October 7, 2015, Beijing suffered the most severe particulate pollution, with mean PM_{2.5} concentrations exceeding 150 $\mu\text{g m}^{-3}$. During the second episode from 14 to 17 October, the most severe pollution occurred in Beijing and the west of Shandong province.

As one of the most important oxidants in the atmosphere, O₃ is an indicator of the AOC (Thompson, 1992). Fig. 5 provides comparisons of the simulated and observed distribution of the average O₃ concentrations in the afternoon (12:00–19:00 LT) during the two severe pollution episodes. The observation shows that the O₃ concentration over BTH is generally more than 100 $\mu\text{g m}^{-3}$ during the two episodes, indicating high AOC. The model reasonably reproduces the observed high O₃ concentrations over BTH, but overestimation also occurs, particularly in

Tianjin. The WRF-Chem model does not perform well in cloud simulations (PaiMazumder, 2012), and is apt to underestimate the cloud fraction over the areas with abundant moisture from underlying surfaces (Fig. S2). The underestimation of cloud fraction in the model results in an overprediction of incident solar radiation, which would facilitate photochemistry and O₃ production rates and contribute to the overestimation of O₃ concentrations.

3.3. Sensitivity experiments

3.3.1. Influence of AOC changes

In consideration of the curial roles of the OH radical and O₃ in AOC (Elshorbagy et al., 2009; Lelieveld et al., 2016; S. C. Liu et al., 1988), we use them as AOC indicators in this study. Fig. 6a presents the variation of the mean nitrate and PM_{2.5} concentrations during the simulation period in Beijing as a function of the OH concentration changes by differentiating the REF and AOC1-5 cases. The decrease in OH concentrations monotonically lowers the nitrate aerosol and PM_{2.5} concentration. As the OH radical (O₃) concentration is decreased by 46.2% (41.0%) in the AOC5 case compared to the REF case, the mean nitrate aerosol and PM_{2.5} concentrations in Beijing are lowered by 18.2% ($7.5 \mu\text{g m}^{-3}$) and 18.9% ($24.7 \mu\text{g m}^{-3}$), respectively, and about 30% of the PM_{2.5} decrease is attributed to the reduction in nitrate aerosols. As a comparison, the observed O₃ concentration has increased by more than 60% in Beijing and nearly 30% in BTH from 2013 to 2015 (Fig. 3) during particulate pollution episodes, showing the potentially important contribution of increasing AOC to the nitrate and PM_{2.5} concentrations. Fig. 7a and b shows the distribution of the changes in nitrate and PM_{2.5} concentrations averaged over the simulation period by differentiating the REF and AOC5 case. In the plain area of BTH, the nitrate and PM_{2.5} concentrations are decreased by more than 5 $\mu\text{g m}^{-3}$ and 10 $\mu\text{g m}^{-3}$, respectively. The largest nitrate and PM_{2.5} decreases occur in the southeastern part of Beijing, reaching 10–20 $\mu\text{g m}^{-3}$ and more than 30 $\mu\text{g m}^{-3}$, respectively. The substantial decreases in nitrate and PM_{2.5} concentrations unveil the important role of AOC in modulating atmospheric chemistry and ambient aerosols.

3.3.2. Effect of SO₂ mitigation

Fig. 6b provides the variations of the mean nitrate, sulfate and PM_{2.5} concentrations during the simulation period in Beijing as a function of the SO₂ concentration changes by differentiating the REF and SUL1-5 cases. Increasing SO₂ emissions leads to an approximately proportional enhancement in sulfate concentrations. A 97.5% increase in SO₂ concentrations results in a 11.2% enhancement in PM_{2.5} concentrations. However, increasing SO₂ enhances the competition of sulfate for base

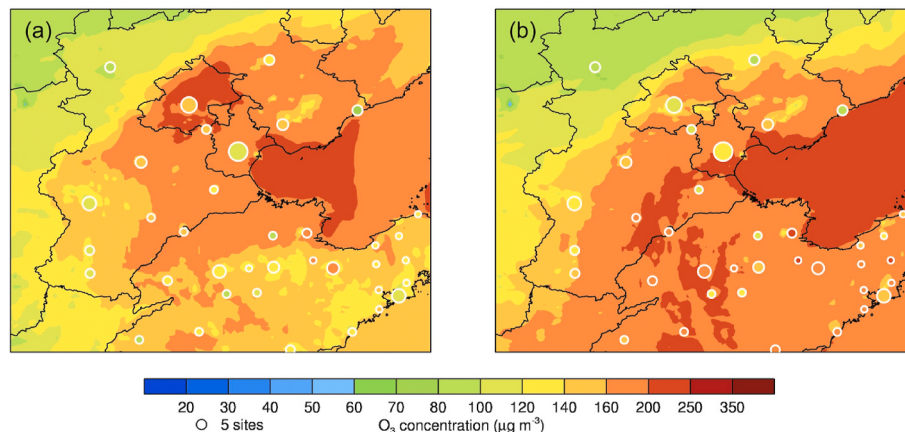


Fig. 5. Spatial distributions of simulated (colored shadings) and observed (colored dots) average O₃ concentrations in the afternoon (12:00–19:00 LT) during the two severe particulate pollution episodes in October 2015. (a) 5–7 October and (b) 14–17 October. The size of the colored dots presents the number of ambient monitoring stations in each city.

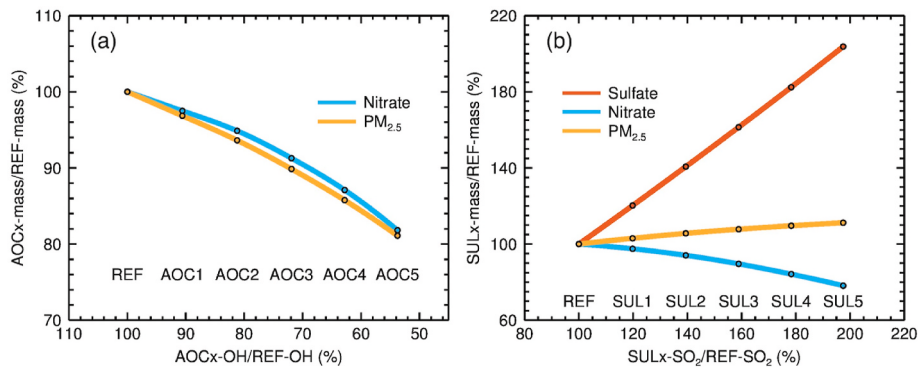


Fig. 6. Impacts of the changes in AOC and SO₂ emissions on ambient aerosols in Beijing. (a) Mass changes of nitrate aerosols and PM_{2.5} concentration caused by the AOC changes. (b) Mass changes of sulfate, nitrate, and PM_{2.5} concentrations due to the changes in SO₂ emissions.

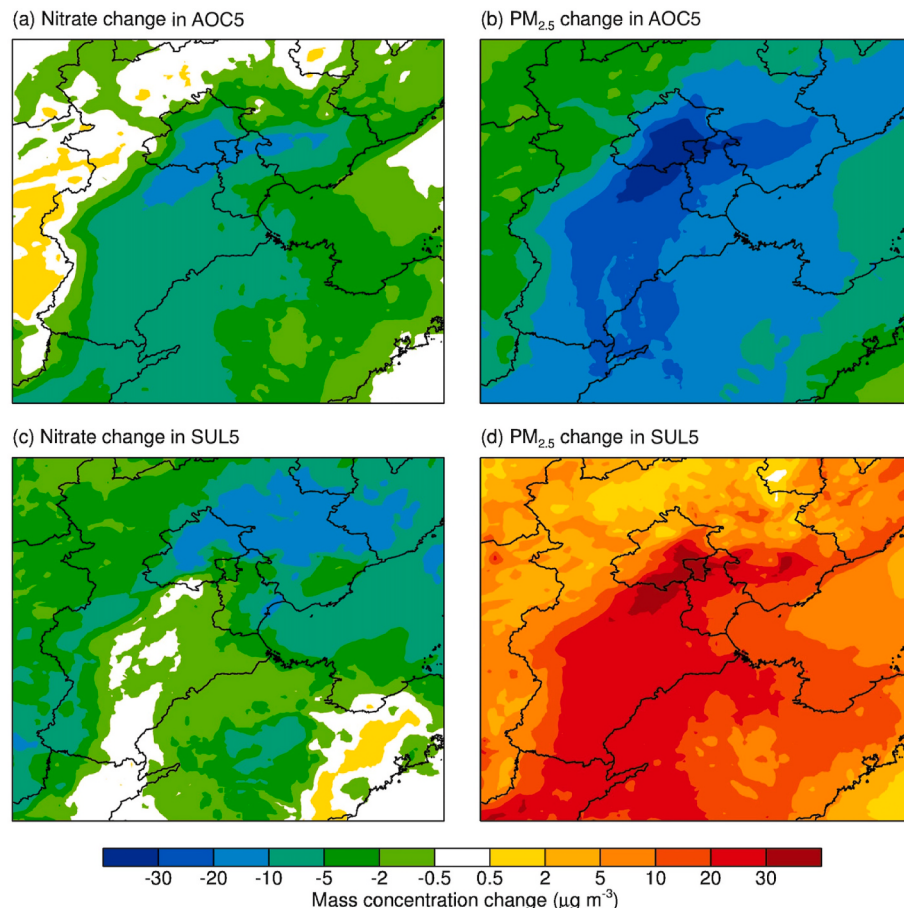


Fig. 7. Spatial impacts of the changes in AOC and SO₂ emissions on ambient aerosols. Mass changes of (a, c) nitrate and (b, d) PM_{2.5} in the AOC5 scenario with a 46.2% (41.0%) decrease in OH (O₃) concentration (a, b) and in the SUL5 scenario with a 100 % increase in SO₂ emission (c, d).

ions, which suppresses nitrate formation (Feng et al., 2018; Lei and Wuebbles, 2013). When SO₂ emissions are increased by 100% in the SUL5 case, sulfate concentrations are elevated by 103.8%, but nitrate concentrations are lowered by 21.9% compared to the REF case. It should be noted that the PM_{2.5} enhancement is mainly attributed to increases in sulfate and is to a certain degree offset by decreases in nitrate. For instance, in the SUL5 case, the average PM_{2.5} concentration in Beijing is increased by 14.6 µg m⁻³ compared to the REF case; meanwhile, the increase in sulfate and decrease in nitrate is about 19.0 µg m⁻³ and 9.0 µg m⁻³, respectively. Fig. 7c and d shows the distribution of the changes in nitrate and PM_{2.5} concentrations averaged over the simulation period by differentiating the REF and SUL5 case, respectively. In the

plain area of BTB, increasing SO₂ emissions generally enhances PM_{2.5} concentrations by more than 10 µg m⁻³, but the PM_{2.5} increase in the northwest part of Beijing and its northeast surrounding areas is not noticeable, less than 5 µg m⁻³, which is caused by the nitrate aerosol decrease over these areas (Fig. 7c-d). Additionally, effects of the sulfate competition on the nitrate formation exhibit a significant spatial variability in BTB, which is modulated by the distribution of ammonia emissions (Feng et al., 2018). Fig. S3 shows that the responses of nitrate and PM_{2.5} concentrations to a 100% increase in SO₂ emission are positively correlated with the NH₃ emission rate over the BTB area during the study period.

4. Conclusions

The ground-based observations show a significant reduction in SO₂ concentration but a remarkable increase in nitrate aerosol and hence persistently high PM_{2.5} levels in Beijing since the strict control on anthropogenic emissions in 2013. From the perspective of atmospheric chemistry, we propose two candidate causes to uncover the mystery: the increasing AOC and the weakening competition between sulfate and nitrate. Using the WRF-Chem model, we examine the roles of proposed candidates in altering nitrate formation and PM_{2.5} concentrations. The results suggest that the enhancing AOC plays a vital role in strengthening nitrate formation which is also the main culprit for the persistently high PM_{2.5} level. In addition, although the effective mitigation of SO₂ emission attenuates PM_{2.5} levels since 2013, the resulting weakened sulfate competition favors nitrate formation and increases nitrate levels.

Based on observation analyses and model experiments, we conclude that the nitrate aerosol has become a dominant contributor to particulate pollution in Beijing, and the increasing AOC and decreasing sulfate competition enhance the nitrate formation. Increase in nitrate aerosols offsets decrease in sulfate aerosols, which sustains the high PM_{2.5} level during particulate pollution episode in Beijing. Our results also suggest that lowering AOC is beneficial to mitigate nitrate and PM_{2.5} concentrations. Since the AOC involves so many chemical species and processes in the atmosphere, further studies need to be conducted to explore optimal ways to decrease the AOC level.

Author contribution

GL designed the research; TF performed the model simulation and wrote the paper; SL provided the measurements of air pollutants in Beijing; SZ, JW, XL, LL, RW, and XZ analyzed the simulation and observation data; NB, XT, and GL revised the paper.

Declaration of competing interest

The authors declare that they have no known competing financial interests or personal relationships that could appear to influence the work reported in this paper.

Acknowledgements

This work was supported by the National Key R&D Plan (Quantitative Relationship and Regulation Principle between Regional Oxidation Capacity of Atmospheric and Air Quality (2017YFC0210000)), the National Natural Science Foundation of China (no. 41703127, 41430424, 41661144020), and the Natural Science Foundation of Zhejiang Province (no. LZ20D050001). This study was also sponsored by K. C. Wong Magna Fund in Ningbo University.

Appendix A. Supplementary data

Supplementary data to this article can be found online at <https://doi.org/10.1016/j.atmosenv.2020.117995>.

References

- Aiken, A.C., DeCarlo, P.F., Kroll, J.H., Worsnop, D.R., Huffman, J.A., Docherty, K.S., Ulbrich, I.M., Mohr, C., Kimmel, J.R., Sueper, D., Sun, Y., Zhang, Q., Trimborn, A., Northway, M., Ziemann, P.J., Canagaratna, M.R., Onasch, T.B., Alfarra, M.R., Prévôt, A.S.H., Dommen, J., Duplissy, J., Metzger, A., Baltensperger, U., Jimenez, J.L., 2008. O/C and OM/OC ratios of primary, secondary, and ambient organic aerosols with high-resolution time-of-flight aerosol mass spectrometry. Environ. Sci. Technol. 42, 4478–4485. <https://doi.org/10.1021/es703009q>.
- Beccaceci, S., McGhee, E.A., Brown, R.J.C., Green, D.C., 2015. A comparison between a semi-continuous analyzer and filter-based method for measuring anion and cation concentrations in PM 10 at an urban background site in London. Aerosol. Sci. Technol. 49, 793–801. <https://doi.org/10.1080/02786826.2015.1073848>.
- Binkowski, F.S., Roselle, S.J., 2003. Models-3 Community Multiscale Air Quality (CMAQ) model aerosol component 1. Model description. J. Geophys. Res. 108, 4183. <https://doi.org/10.1029/2001JD001409>.
- Cai, S., Wang, Y., Zhao, Bin, Wang, S., Chang, X., Hao, J., 2017. The impact of the “air pollution prevention and control action plan” on PM_{2.5} concentrations in jing-jin-ji region during 2012–2020. Sci. Total Environ. 580, 197–209. <https://doi.org/10.1016/j.scitotenv.2016.11.188>.
- Cao, J., Wang, Q.Y., Chow, J.C., Watson, J.G., Tie, X.X., Shen, Z.X., Wang, P., An, Z.S., 2012a. Impacts of aerosol compositions on visibility impairment in Xi'an, China. Atmos. Environ. 59, 559–566. <https://doi.org/10.1016/j.atmosenv.2012.05.036>.
- Cao, J., Xu, H., Xu, Q., Chen, B., Kan, H., 2012b. Fine particulate matter constituents and cardiopulmonary mortality in a heavily polluted Chinese city. Environ. Health Perspect. 120, 373–378. <https://doi.org/10.1289/ehp.1103671>.
- Chen, F., Dudhia, J., 2001. Coupling an advanced land surface-hydrology model with the Penn State-NCAR MM5 modeling system. Part II: preliminary model validation. doi: 10.1175/1520-0493(2001)129<0569:caalsh>2.0.co;2 Mon. Weather Rev. 129, 569–585.
- Chen, S., Wang, H., Lu, K., Zeng, L., Hu, M., Zhang, Y., 2020. The trend of surface ozone in Beijing from 2013 to 2019: indications of the persisting strong atmospheric oxidation capacity. Atmos. Environ. 242, 117801–117808. <https://doi.org/10.1016/j.atmosenv.2020.117801>.
- Cheng, N., Li, Y., Zhang, D., Chen, T., Sun, F., Chen, C., Meng, F., 2016. Characteristics of ground ozone concentration over Beijing from 2004 to 2015: trends, transport, and effects of reductions. Atmos. Chem. Phys. Discuss. 1–21. <https://doi.org/10.5194/acp-2016-508>.
- Chou, M.-D., Suarez, M.J., 1999. A Solar Radiation Parameterization for Atmospheric Studies (No. NASA/TM-1999-10460), NASA Technique Report.
- Chou, M.-D., Suarez, M.J., Liang, X.-Z., Yan, M.M.H., 2001. A Thermal Infrared Radiation Parameterizer for Atmospheric Studies (No. NASA/TM-2001-104606), NASA Technique Report.
- Donahue, N.M., Robinson, A.L., Stanier, C.O., Pandis, S.N., 2006. Coupled partitioning, dilution, and chemical aging of semivolatile organics. Environ. Sci. Technol. 40, 2635–2643. <https://doi.org/10.1021/es052297c>.
- Elshorbany, Y.F., Kurtenbach, R., Wiesen, P., Lissi, E., Rubio, M., Villena, G., Gramsch, E., Rickard, A.R., Pilling, M.J., Kleffmann, J., 2009. Oxidation capacity of the city air of Santiago, Chile. Atmos. Chem. Phys. 9, 2257–2273. <https://doi.org/10.5194/acp-9-2257-2009>.
- Feng, T., Bei, N., Zhao, S., Wu, J., Li, X., Zhang, T., Cao, J., Zhou, W., Li, G., 2018. Wintertime nitrate formation during haze days in the Guanzhong basin, China: a case study. Environ. Pollut. 243, 1057–1067. <https://doi.org/10.1016/j.envpol.2018.09.069>.
- Feng, T., Li, G., Cao, J., Bei, N., Shen, Z., Zhou, W., Liu, S., Zhang, T., Wang, Y., Huang, R.-J., Tie, X., Molina, L.T., 2016. Simulations of organic aerosol concentrations during springtime in the Guanzhong Basin, China. Atmos. Chem. Phys. 16, 10045–10061. <https://doi.org/10.5194/acp-16-10045-2016>.
- Feng, T., Zhao, S., Bei, N., Wu, J., Liu, S., Li, X., Liu, L., Qian, Y., Yang, Q., Wang, Y., Zhou, W., Cao, J., Li, G., 2019. Secondary organic aerosol enhanced by increasing atmospheric oxidizing capacity in Beijing-Tianjin-Hebei (BTH), China. Atmos. Chem. Phys. 19, 7429–7443. <https://doi.org/10.5194/acp-19-7429-2019>.
- Grell, G.A., Peckham, S.E., Schmitz, R., McKeen, S.A., Frost, G., Skamarock, W.C., Eder, B., 2005. Fully coupled “online” chemistry within the WRF model. Atmos. Environ. 39, 6957–6975. <https://doi.org/10.1016/j.atmosenv.2005.04.027>.
- Guenther, A., Karl, T., Harley, P., Wiedinmyer, C., Palmer, P.I., Geron, C., 2006. Estimates of global terrestrial isoprene emissions using MEGAN (model of emissions of gases and aerosols from nature). Atmos. Chem. Phys. 6, 3181–3210. <https://doi.org/10.5194/acp-6-3181-2006>.
- He, K., Yang, F., Ma, Y., Zhang, Q., Yao, X., Chan, C.K., Cadle, S., Chan, T., Mulawa, P., 2001. The characteristics of PM_{2.5} in Beijing, China. Atmos. Environ. 35, 4959–4970. [https://doi.org/10.1016/S1352-2310\(01\)00301-6](https://doi.org/10.1016/S1352-2310(01)00301-6).
- He, K., Zhang, Q., Hong, C., Xie, T., Bai, Y., Du, J., Zhao, L., Cai, J., Lin, Y., Zhou, R., 2017. Can Beijing, Tianjin and Hebei Achieve Their PM_{2.5} Targets by 2017? Clean Air Alliance of China, Beijing.
- Hong, S.Y., Lim, J., 2006. The WRF single-moment 6-class microphysics scheme (WSM6). Asia-Pac. J. Atmos. Sci. 42, 129–151.
- Horowitz, L.W., Walters, S., Mauzerall, D.L., Emmons, L.K., Rasch, P.J., Granier, C., Tie, X., Lamarque, J.-F., Schultz, M.G., Tyndall, G.S., Orlando, J.H., Brasseur, G.P., 2003. A global simulation of tropospheric ozone and related tracers: description and evaluation of MOZART, version 2. J. Geophys. Res. 108, 4784. <https://doi.org/10.1029/2002jd002853>.
- Huang, R.-J., Zhang, Y., Bozzetti, C., Ho, K.F., Cao, J., Han, Y., Daellenbach, K.R., Slowik, J.G., Platt, S.M., Canonaco, F., Zotter, P., Wolf, R., Pieber, S.M., Bruns, E.A., Crippa, M., Cairelli, G., Piazzalunga, A., Schwikowski, M., Abbaszade, G., Schnelle-Kreis, J., Zimmermann, R., An, Z., Szidat, S., Baltensperger, U., Haddad, El, I., Prévôt, A.S.H., 2014. High secondary aerosol contribution to particulate pollution during haze events in China. Nature 514, 218–222. <https://doi.org/10.1038/nature13774>.
- Janjić, Z.I., 2002. Nonsingular Implementation of the Mellor-Yamada Level 2.5 Scheme in the NCEP Meso Model (No. 437). NCEP office note.
- Lei, H., Huebbles, D.J., 2013. Chemical competition in nitrate and sulfate formations and its effect on air quality. Atmos. Environ. 80, 472–477. <https://doi.org/10.1016/j.atmosenv.2013.08.036>.
- Lelieveld, J., Gromov, S., Pozzer, A., Taraborrelli, D., 2016. Global tropospheric hydroxyl distribution, budget and reactivity. Atmos. Chem. Phys. 16, 12477–12493. <https://doi.org/10.5194/acp-16-12477-2016>.
- Li, G., Bei, N., Cao, J., Wu, J., Long, X., Feng, T., Dai, W., Liu, S., Zhang, Q., Tie, X., 2017a. Widespread and persistent ozone pollution in eastern China during the non-

- winter season of 2015: observations and source attributions. *Atmos. Chem. Phys.* 17, 2759–2774. <https://doi.org/10.5194/acp-17-2759-2017>.
- Li, G., Bei, N., Tie, X., Molina, L.T., 2011a. Aerosol effects on the photochemistry in Mexico City during MCMA-2006/MILAGRO campaign. *Atmos. Chem. Phys.* 11, 5169–5182. <https://doi.org/10.5194/acp-11-5169-2011>.
- Li, G., Lei, W., Bei, N., Molina, L.T., 2012. Contribution of garbage burning to chloride and $\text{PM}_{2.5}$ in Mexico City. *Atmos. Chem. Phys.* 12, 8751–8761. <https://doi.org/10.5194/acp-12-8751-2012>.
- Li, G., Lei, W., Zavala, M., Volkamer, R., Dusander, S., Stevens, P., Molina, L.T., 2010. Impacts of HONO sources on the photochemistry in Mexico city during the MCMA-2006/MILAGRO campaign. *Atmos. Chem. Phys.* 10, 6551–6567. <https://doi.org/10.5194/acp-10-6551-2010>.
- Li, G., Wang, Y., Lee, K.-H., Diao, Y., Zhang, R., 2009. Impacts of aerosols on the development and precipitation of a mesoscale squall line. *J. Geophys. Res.* 114, D17205. <https://doi.org/10.1029/2008JD011581>.
- Li, G., Zavala, M., Lei, W., Tsimplidi, A.P., Karydis, V.A., Pandis, S.N., Canagaratna, M.R., Molina, L.T., 2011b. Simulations of organic aerosol concentrations in Mexico City using the WRF-CHEM model during the MCMA-2006/MILAGRO campaign. *Atmos. Chem. Phys.* 11, 3789–3809. <https://doi.org/10.5194/acp-11-3789-2011>.
- Li, H., Zhang, Q., Zheng, B., Chen, C., Wu, N., Guo, H., Zhang, Y., Zheng, Y., Li, X., He, K., 2018. Nitrate-driven urban haze pollution during summertime over the North China Plain. *Atmos. Chem. Phys.* 18, 5293–5306. <https://doi.org/10.5194/acp-18-5293-2018>.
- Li, K., Jacob, D.J., Liao, H., Shen, L., Zhang, Q., Bates, K.H., 2018. Anthropogenic drivers of 2013–2017 trends in summer surface ozone in China. *Proc. Natl. Acad. Sci. U.S.A.* 17 <https://doi.org/10.1073/pnas.1812168116>, 201812168–6.
- Li, M., Zhang, Q., Kurokawa, J.-I., Woo, J.-H., He, K., Lu, Z., Ohara, T., Song, Y., Streets, D.G., Carmichael, G.R., Cheng, Y., Hong, C., Huo, H., Jiang, X., Kang, S., Liu, F., Su, H., Zheng, B., 2017b. MIX: a mosaic Asian anthropogenic emission inventory under the international collaboration framework of the MICS-Asia and HTAP. *Atmos. Chem. Phys.* 17, 935–963. <https://doi.org/10.5194/acp-17-935-2017>.
- Liu, S.C., Cox, R.A., Crutzen, P.J., Ehhalt, D.H., Guicherit, R., Hofzumahaus, A., Kley, D., Penkett, S.A., Phillips, L.F., Poppe, D., Rowland, F.S., 1988. Group report: oxidizing capacity of the atmosphere. In: Rowland, F.S., Isaksen, I.S.A. (Eds.), *The Changing Atmosphere*, pp. 219–232. Chichester, UK.
- Liu, W., Shen, G., Chen, Y., Shen, H., Huang, Y., Li, T., Wang, Y., Fu, X., Tao, S., Liu, W., Huang-Fu, Y., Zhang, W., Xue, C., Liu, G., Wu, F., Wong, M., 2018. Air pollution and inhalation exposure to particulate matter of different sizes in rural households using improved stoves in central China. *J. Environ. Sci.* 63, 87–95. <https://doi.org/10.1016/j.jes.2017.06.019>.
- Ma, Z., Xu, J., Quan, W., Zhang, Z., Lin, W., Xu, X., 2016. Significant increase of surface ozone at a rural site, north of eastern China. *Atmos. Chem. Phys.* 16, 3969–3977. <https://doi.org/10.5194/acp-16-3969-2016>.
- Morgan, W.T., Allan, J.D., Bower, K.N., Esselborn, M., Harris, B., Henzing, J.S., Highwood, E.J., Kiendler-Scharr, A., McMeeking, G.R., Mensah, A.A., Northway, M.J., Osborne, S., Williams, P.I., Krejci, R., Coe, H., 2010. Enhancement of the aerosol direct radiative effect by semi-volatile aerosol components: airborne measurements in North-Western Europe. *Atmos. Chem. Phys.* 10, 8151–8171. <https://doi.org/10.5194/acp-10-8151-2010>.
- Nenes, A., Pandis, S.N., Pilinis, C., 1998. ISORROPIA: a new thermodynamic equilibrium model for multiphase multicomponent inorganic aerosols. *Aquat. Geochem.* 4, 123–152. <https://doi.org/10.1023/A:1009604003981>.
- PaiMazumder, D., 2012. Evaluation of WRF-forecasts over siberia: air mass formation, clouds and precipitation. *Open Atmos. Sci. J.* 6, 93–110. <https://doi.org/10.2174/1874282301206010093>.
- Poulain, L., Spindler, G., Birmili, W., Plass-Dümler, C., Wiedensohler, A., Herrmann, H., 2011. Seasonal and diurnal variations of particulate nitrate and organic matter at the Ift research station Melpitz. *Atmos. Chem. Phys.* 11, 12579–12599. <https://doi.org/10.5194/acp-11-12579-2011>.
- Robinson, A.L., Donahue, N.M., Shrivastava, M.K., Weitkamp, E.A., Sage, A.M., Grieshop, A.P., Lane, T.E., Pierce, J.R., Pandis, S.N., 2007. Rethinking organic aerosols: semivolatile emissions and photochemical aging. *Science* 315, 1259–1262. <https://doi.org/10.1126/science.1133061>.
- Seinfeld, J.H., Pandis, S.N., 2006. *Atmospheric Chemistry and Physics - from Air Pollution to Climate Change*, second ed. John Wiley & Sons, New Jersey.
- Stein, A.F., Saylor, R.D., 2012. Sensitivities of sulfate aerosol formation and oxidation pathways on the chemical mechanism employed in simulations. *Atmos. Chem. Phys.* 12, 8567–8574. <https://doi.org/10.5194/acp-12-8567-2012>.
- Sun, Y., Wang, Z., Dong, H., Yang, T., Li, J., Pan, X., Chen, P., Jayne, J.T., 2012. Characterization of summer organic and inorganic aerosols in Beijing, China with an aerosol chemical speciation monitor. *Atmos. Environ.* 51, 250–259. <https://doi.org/10.1016/j.atmosenv.2012.01.013>.
- Sun, Y.L., Wang, Z.F., Fu, P.Q., Yang, T., Jiang, Q., Dong, H.B., Li, J., Jia, J.J., 2013. Aerosol composition, sources and processes during wintertime in Beijing, China. *Atmos. Chem. Phys.* 13, 4577–4592. <https://doi.org/10.5194/acp-13-4577-2013>.
- Thompson, A.M., 1992. The oxidizing capacity of the earth's atmosphere: probable past and future changes. *Science* 256, 1157–1165. <https://doi.org/10.1126/science.256.5060.1157>.
- Tie, X., Huang, R.-J., Dai, W., Cao, J., Long, X., Su, X., Zhao, S., Wang, Q., Li, G., 2016. Effect of heavy haze and aerosol pollution on rice and wheat productions in China. *Sci. Rep.* 1–6. <https://doi.org/10.1038/srep29612>.
- Tie, X., Madronich, S., Walters, S., Zhang, R., Rasch, P., Collins, W., 2003. Effect of clouds on photolysis and oxidants in the troposphere. *J. Geophys. Res.* 108, 4642. <https://doi.org/10.1029/2003JD003659>.
- Twigg, M.M., Di Marco, C.F., Leeson, S., van Dijk, N., Jones, M.R., Leith, I.D., Morrison, E., Coyle, M., Proost, R., Peeters, A.N.M., Lemon, E., Frelink, T., Braban, C. F., Nemitz, E., Cape, J.N., 2015. Water soluble aerosols and gases at a UK background site – Part 1: controls of PM 2.5 and PM 10 aerosol composition. *Atmos. Chem. Phys.* 15, 8131–8145. <https://doi.org/10.5194/acp-15-8131-2015>.
- Wang, G., Zhang, R., Gomez, M.E., Yang, L., Levy Zamora, M., Hu, M., Lin, Y., Peng, J., Guo, S., Meng, J., Li, J., Cheng, C., Hu, T., Ren, Y., Wang, Y., Gao, J., Cao, J., An, Z., Zhou, W., Li, G., Wang, J., Tian, P., Marrero-Ortiz, W., Secret, J., Du, Z., Zheng, J., Shang, D., Zeng, L., Shao, M., Wang, W., Huang, Y., Wang, Y., Zhu, Y., Li, Y., Hu, J., Pan, B., Cai, L., Cheng, Y., Ji, Y., Zhang, F., Rosenfeld, D., Liss, P.S., Duce, R.A., Kolb, C.E., Molina, M.J., 2016. Persistent sulfate formation from London Fog to Chinese haze. *Proc. Natl. Acad. Sci. U.S.A.* 201616540–18 <https://doi.org/10.1073/pnas.1616540113>.
- Wei, F., Teng, E., Wu, G., Hu, W., Wilson, W.E., Chapman, R.S., Pau, J.C., Zhang, J., 1999. Ambient concentrations and elemental compositions of PM10 and PM2.5 in four Chinese cities. *Environ. Sci. Technol.* 33, 4188–4193. <https://doi.org/10.1021/es990494a>.
- Wei, S., Shen, G., Zhang, Y., Xue, M., Xie, H., Lin, P., Chen, Y., Wang, X., Tao, S., 2014. Field measurement on the emissions of PM, OC, EC and PAHs from indoor crop straw burning in rural China. *Environ. Pollut.* 184, 18–24. <https://doi.org/10.1016/j.envpol.2013.07.036>.
- Wen, L., Xue, L., Wang, X., Xu, C., Chen, T., Yang, L., Wang, T., Zhang, Q., Wang, W., 2018. Summertime fine particulate nitrate pollution in the North China Plain: increasing trends, formation mechanisms and implications for control policy. *Atmos. Chem. Phys.* 18, 11261–11275. <https://doi.org/10.5194/acp-18-11261-2018>.
- Wesely, M.L., 1989. Parameterization of surface resistances to gaseous dry deposition in regional-scale numerical models. *Atmos. Environ.* 23, 1293–1304. [https://doi.org/10.1016/0004-6981\(89\)90153-4](https://doi.org/10.1016/0004-6981(89)90153-4).
- Willmott, C.J., 1981. On the validation of models. *Phys. Geogr.* 2, 184–194. <https://doi.org/10.1080/02723646.1981.10642213>.
- Wu, J., Bei, N., Hu, B., Liu, S., Zhou, M., Wang, Q., Li, X., Liu, L., Feng, T., Liu, Z., Wang, Y., Cao, J., Tie, X., Wang, J., Molina, L.T., Li, G., 2019. Aerosol-radiation feedback deteriorates the wintertime haze in the North China Plain. *Atmos. Chem. Phys.* 19, 8703–8719. <https://doi.org/10.5194/acp-19-8703-2019>.
- Wu, J., Li, G., Cao, J., Bei, N., Wang, Y., Feng, T., Huang, R., Liu, S., Zhang, Q., Tie, X., 2017. Contributions of trans-boundary transport to summertime air quality in Beijing, China. *Atmos. Chem. Phys.* 17, 2035–2051. <https://doi.org/10.5194/acp-17-2035-2017>.
- Xing, L., Fu, T.M., Cao, J.J., Lee, S.C., Wang, G.H., Ho, K.F., Cheng, M.C., You, C.F., Wang, T.J., 2013. Seasonal and spatial variability of the OM/OC mass ratios and high regional correlation between oxalic acid and zinc in Chinese urban organic aerosols. *Atmos. Chem. Phys.* 13, 4307–4318. <https://doi.org/10.5194/acp-13-4307-2013>.
- Zhang, H., Wang, S., Hao, J., Wang, X., Wang, S., Chai, F., Li, M., 2016. Air pollution and control action in Beijing. *J. Clean. Prod.* 112, 1519–1527. <https://doi.org/10.1016/j.jclepro.2015.04.092>.
- Zhang, Q., Quan, J., Tie, X., Li, X., Liu, Q., Gao, Y., Zhao, D., 2015. Effects of meteorology and secondary particle formation on visibility during heavy haze events in Beijing, China. *Sci. Total Environ.* 502, 578–584. <https://doi.org/10.1016/j.scitotenv.2014.09.079>.
- Zhang, Q., Streets, D.G., Carmichael, G.R., 2009. Asian emissions in 2006 for the NASA INTEX-B mission. *Atmos. Chem. Phys.* 9, 5131–5153. <https://doi.org/10.5194/acp-9-5131-2009>.
- Zhang, R., Jing, J., Tao, J., Hsu, S.C., Wang, G., Cao, J., Lee, C.S.L., Zhu, L., Chen, Z., Zhao, Y., Shen, Z., 2013. Chemical characterization and source apportionment of $\text{PM}_{2.5}$ in Beijing: seasonal perspective. *Atmos. Chem. Phys.* 13, 7053–7074. <https://doi.org/10.5194/acp-13-7053-2013>.
- Zhang, R., Li, G., Fan, J., Wu, D.L., Molina, M.J., 2007. Intensification of Pacific storm track linked to Asian pollution. *Proc. Natl. Acad. Sci. U.S.A.* 104, 5295–5299. <https://doi.org/10.1073/pnas.0700618104>.
- Zhang, Y.-L., Cao, F., 2015. Fine particulate matter ($\text{PM}_{2.5}$) in China at a city level. *Sci. Rep.* 1–12. <https://doi.org/10.1038/srep14884>.
- Zhao, S., Zhang, H., Wang, Z., Jing, X., 2017. Simulating the effects of anthropogenic aerosols on terrestrial aridity using an aerosol-climate coupled model. *J. Clim.* 30, 7451–7463. <https://doi.org/10.1175/JCLI-D-16-0407.1>.
- Zheng, B., Tong, D., Li, M., Liu, F., Hong, C., Geng, G., Li, H., Li, X., Peng, L., Qi, J., Yan, L., Zhang, Y., Zhao, H., Zheng, Y., He, K., Zhang, Q., 2018. Trends in China's anthropogenic emissions since 2010 as the consequence of clean air actions. *Atmos. Chem. Phys.* 18, 14095–14111. <https://doi.org/10.5194/acp-18-14095-2018>.
- Zheng, G.J., Duan, F.K., Su, H., Ma, Y.L., Cheng, Y., Zheng, B., Zhang, Q., Huang, T., Kimoto, T., Chang, D., Pöschl, U., Cheng, Y.F., He, K.B., 2015. Exploring the severe winter haze in Beijing: the impact of synoptic weather, regional transport and heterogeneous reactions. *Atmos. Chem. Phys.* 15, 2969–2983. <https://doi.org/10.5194/acp-15-2969-2015>.
- Zhou, X., Bei, N., Liu, H., Cao, J., Xing, L., Lei, W., Molina, L.T., Li, G., 2017. Aerosol effects on the development of cumulus clouds over the Tibetan Plateau. *Atmos. Chem. Phys.* 17, 7423–7434. <https://doi.org/10.5194/acp-17-7423-2017>.